INTERNATIONAL JOURNAL FOR NUMERICAL METHODS IN FLUIDS
Int. J. Numer. Meth. Fluids 2008; **56**:1399–1407
Published online 17 December 2007 in Wiley InterScience (www.interscience.wiley.com). DOI: 10.1002/fld.1709

Numerical solution of 2D and 3D viscous incompressible steady and unsteady flows using artificial compressibility method

P. Louda[1,*,†], K. Kozel[1] and J. Příhoda[2]

[1]*Department of Technical Mathematics, FME, Czech Technical University, Karlovo nám. 13, 12135 Praha 2, Czech Republic*
[2]*Institute of Thermomechanics, Dolejškova 5, Praha 8, Czech Republic*

SUMMARY

In this work, artificial compressibility method is used to solve steady and unsteady flows of viscous incompressible fluid. The method is based on implicit higher-order upwind discretization of Navier–Stokes equations. The extension for unsteady simulation is considered by increasing artificial compressibility parameter or by using dual time stepping. Turbulence models are eddy-viscosity SST model and explicit algebraic Reynolds stress model. Results for steady turbulent flow over confined backward-facing step, unsteady laminar flow around circular cylinder and for unsteady turbulent free synthetic jet are presented.

Received 25 April 2007; Revised 7 November 2007; Accepted 7 November 2007

KEY WORDS: artificial compressibility; dual time; backward-facing step; synthetic jet; turbulence model; SST; EARSM

1. INTRODUCTION

The work deals with numerical solution of 3D incompressible viscous (laminar and turbulent) flows. Solving viscous incompressible flows modelled by the system of Navier–Stokes (NS) equations one can find firstly velocity vector $(u, v, w)^{n+1}$ using numerical solution of momentum equations with $p = p^n$ and then solving corresponding Poisson's equation for p^{n+1} using new velocity $(u, v, w)^{n+1}$ on the right-hand side of Poisson's equation. One of these methods authors used in [1]. The methods with pressure Poisson equation for unsteady simulations generally are limited in time accuracy, especially if they are implicit. On the other hand for application of advanced turbulence

*Correspondence to: P. Louda, Department of Technical Mathematics, FME, Czech Technical University, Karlovo nám. 13, 12135 Praha 2, Czech Republic.
†E-mail: louda@marian.fsik.cvut.cz

Contract/grant sponsor: GA CR and Research plan MSM 6840770010; contract/grant number: 201/05/0005

models that are integrated up to the wall and require refined meshes in the boundary layer, the implicit discretization is highly useful. The other problem of this approach is the solution of Poisson's equation itself. In this work, the authors use structured multi-block non-orthogonal non-regular grids. For such grids, the convergence of a Poisson solver could deteriorate compared with orthogonal one block grid. Therefore, it seems practical to consider the approach based on artificial compressibility both for steady and unsteady simulations. The idea, proposed by Chorin [2], is to complete continuity equation by a pressure time derivative $(1/\beta^2)\partial p/\partial t$ and then, because the whole inviscid system has the form of the system of compressible Euler equations (non-linear hyperbolic system), one can use some numerical scheme for compressible flow computation. With steady boundary conditions and time-dependent method, steady solution may be achieved for $t \to \infty$. In this work, the discretization is implicit using cell-centered finite volume method. An extension for unsteady simulation is achieved by introducing dual time and using implicit discretization for both physical and artificial time.

2. MATHEMATICAL MODEL

A convenient time-marching algorithm for NS equations for incompressible flow (density $\rho = \text{const}$) can be realized by artificial compressibility method [2]. In its simplest form, only the continuity equation is modified by the first term in the following equation:

$$\frac{1}{\beta^2}\frac{\partial(p/\rho)}{\partial t} + \frac{\partial u_1}{\partial x_1} + \frac{\partial u_2}{\partial x_2} + \frac{\partial u_3}{\partial x_3} = 0 \tag{1}$$

where β is a positive parameter. The inviscid part of modified NS equations is now strongly hyperbolic and can be solved by standard methods for hyperbolic conservation laws. The system including the modified continuity equation and the momentum equations can be expressed as

$$\begin{gathered}\Gamma\frac{\partial W}{\partial t} + Rez(W) = 0, \quad \Gamma = \text{diag}[\beta^{-2}, 1, 1, 1], \quad W = \text{col}[p/\rho, u_1, u_2, u_3] \\ (x_1, x_2, x_3) \in D, \quad t \in (0, \infty)\end{gathered} \tag{2}$$

where W is a vector of unknown kinematic pressure and velocity components, and steady residual $Rez(W)$ contains all inviscid and viscous terms. However, the divergence-free velocity field is not achieved before steady state, $\partial p/\partial t = 0$. In unsteady case, the velocity divergence error may have negligible impact on relevant flow parameters if the β^2 is large enough. Other possibility to obtain unsteady solution is to introduce artificial (dual, iterative) time τ and apply the artificial compressibility method in the artificial time:

$$\begin{gathered}\Gamma\frac{\partial W}{\partial \tau} + Rez^{\text{uns}}(W) = 0, \quad Rez^{\text{uns}}(W) = R\frac{\partial W}{\partial t} + Rez(W), \quad R = \text{diag}[0, 1, 1, 1] \\ (x_1, x_2, x_3) \in D, \quad t \in (t_n, t_{n+1}), \quad \tau \in (0, \infty)\end{gathered} \tag{3}$$

where $Rez^{\text{uns}}(W)$ is unsteady residual. The steady state in τ should now be achieved at each physical time level t.

DOI: 10.1002/fld

2.1. Turbulence modelling

In order to simulate turbulent flows, the Reynolds averaging procedure is used. For unsteady simulation it can be understood as phase averaging since the simulated flows have periodic 'steady' state. The Reynolds-averaged equations formally differ from NS equations by additional momentum transport expressed by Reynolds stress tensor. In this work, the Reynolds stress is modelled using SST [3] and explicit algebraic Reynolds stress model (EARSM) turbulence model [4, 5]. In the SST model, the extended eddy-viscosity assumption is used to express the Reynolds stress, while in EARSM a constitutive relation contains terms up to fourth order in terms of velocity gradient. Both turbulence models require solving a system of k–ω equations for turbulent scales.

3. NUMERICAL METHOD

The stability limitation of an explicit scheme for inviscid part requires $\Delta t \sim \Delta s/(u_s + \sqrt{u_s^2 + \beta^2})$, where u_s is flow velocity and Δs grid spacing. It becomes more severe as β increases. The choice of β is problem dependent, there is no general optimum procedure. For robustness, it is recommended [6] that the β be constant for the whole solution domain, although in general the choice should depend on local grid and local convergence rate. In the authors experience with constant β, for orthogonal grids the convergence, e.g. in L_2 norm for pressure is as fast as the one for other unknowns (velocity components) and the steady residual level easily is machine zero even for highly refined grids. For non-orthogonal grids, the pressure residual settles on higher steady value than the other residuals. This, however, does not seem to affect the accuracy of velocity field. The authors choose the β in order of magnitude of maximum flow velocity in the solution domain for steady simulations.

The time discretization schemes considered here are implicit. This choice has several motivations. The low-Re turbulence models require refined grid in the boundary layer, which would limit the time step in an explicit scheme to impractically small value for the viscous stability reason. In single time method, the choice enables larger values of β for unsteady simulation. For the dual time method, the implicit discretization removes dependency between the size of physical and artificial time step.

In ingle time method for steady simulations, the first-order accurate backward Euler scheme is used

$$\Gamma \frac{W_{i,j,k}^{n+1} - W_{i,j,k}^{n}}{\Delta t} + Rez(W)_{i,j,k}^{n+1} = 0 \tag{4}$$

In single time method for unsteady simulations, a second-order accurate three-layer scheme is used instead:

$$\Gamma \frac{3W_{i,j,k}^{n+1} - 4W_{i,j,k}^{n} + W_{i,j,k}^{n-1}}{2\Delta t} + Rez(W)_{i,j,k}^{n+1} = 0 \tag{5}$$

For dual time method, the scheme is a combination of the above two—backward Euler method in artificial time (superscript v) and three-layer scheme for physical time (superscript n)

$$\Gamma \frac{W_{i,j,k}^{v+1} - W_{i,j,k}^{v}}{\Delta \tau} + R \frac{3W_{i,j,k}^{v+1} - 4W_{i,j,k}^{n} + W_{i,j,k}^{n-1}}{2\Delta t} + Rez(W)_{i,j,k}^{v+1} = 0 \tag{6}$$

DOI: 10.1002/fld

The steady residuals are computed by a cell-centered finite volume method with quadrilateral or hexahedral finite volumes in 2D or 3D case, respectively. The discretization of convective terms uses third-order accurate upwind interpolation. Pressure gradient is computed by central approximation. The viscous terms are approximated using second-order central scheme, with cell face derivatives computed on a dual grid of finite volumes constructed over each face of primary grid. The discrete expression for residual is linearized with respect to unknown vector W in each finite volume from the stencil, by means of Newton method. The derivatives are computed analytically. Only five (2D) or seven (3D) finite volumes are retained in the implicit discrete operator. The resulting linear system is thus five or seven block diagonal. The solution is found by a line relaxation method with direct method for block tri-diagonal matrix inversion. The two turbulence model equations are solved decoupled from NS equations and the discretization is same as for the NS equations. Only the negative part of source terms is linearized and included into the implicit operator. Also in EARSM model, only the linear part of Reynolds stresses is treated implicitly, while the higher-order terms are taken from previous time level.

4. NUMERICAL RESULTS

4.1. Steady 2D and 3D turbulent backward-facing step flow

The case of confined backward-facing step was measured by Armaly *et al.* [7]. In the simulation the width of channel is truncated to $6h$, where h is step height. The inlet flow was obtained by separate simulation of fully developed channel flow on the same grid. The computed secondary flow in the inlet is shown in Figure 1 in the form of velocity vectors (note that the vectors for SST model are more magnified). The EARSM model predicts secondary corner vortices, whereas the eddy-viscosity SST predicts no secondary vortices. We compare recirculation length by 2D simulation with 3D results in the center plane in the Table I. The velocity profiles in center plane are shown for both turbulence models in Figure 2.

4.2. Unsteady 2D laminar flow around circular cylinder

In this section, we consider 2D laminar unsteady flow over a circular cylinder placed either in a channel or in a free space. An example of the multi-block grid is shown in Figure 3.

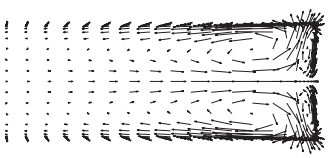

Figure 1. Inlet secondary flow, EARSM turbulence model.

Table I. Length of separation zone in 2D and 3D cases.

	Armaly *et al.*	SST model	EARSM model
2D	—	$8.40h$	$8.52h$
3D	$8h$	$6.70h$	$8.22h$

DOI: 10.1002/fld

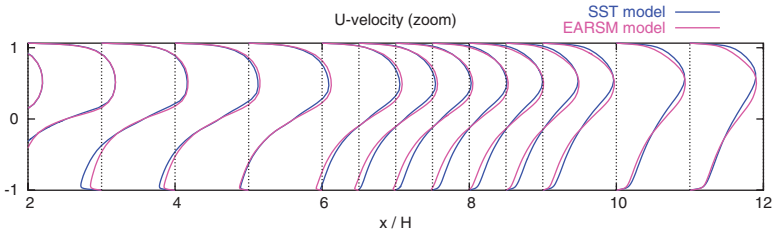

Figure 2. Velocity profiles in the mid-plane.

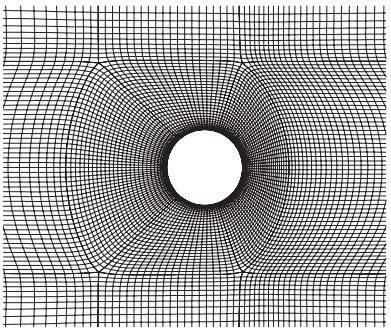

Figure 3. Multi-block grid around a cylinder.

The results of first test case for Reynolds number $Re = UD/v = 100$ and single time method are shown in Figure 4, in the form of drag and lift coefficients C_D, C_L. The Strouhal number of vortex shedding $St = Df/U$, where f is frequency, is $St = 0.288$, below values indicated by [8]. The results improve with increasing value of β, however, the $\beta = 10U$ is about the maximum for a reasonable time step in this case ($\Delta t = 0.02D/U$). Results of dual time stepping method using $\beta = U$, $\Delta t = 0.06D/U$ are shown in Figure 4. The Strouhal number $St = 0.294$. The instantaneous flow field for dual time stepping scheme is shown in Figure 5. Next we show results for second test case achieved by dual time method with $\beta = U, \Delta t = 0.06D/U$. Figure 6 shows Strouhal *vs* Reynolds number in comparison with empirical correlation $St = 0.266 - 1.016/\sqrt{Re}$ [9]. The critical Reynolds number when vortex shedding starts is $Re = 47.5 \pm 0.7$ [9]. In our computation, the flow is steady for $Re = 30$, unsteady but non-periodic for $Re = 40$ and periodic at $Re = 47$. However, for lower Re the computed shedding frequency is higher than the empirical correlation suggests. The evolution of steady and unsteady residual is shown in Figure 7 ($Re = 100$).

4.3. Turbulent 3D synthetic free jet flow

In this part, we consider the synthetic jet generated by periodical inflow/outflow with zero mean value in the circular nozzle [10]. The Reynolds number from nozzle diameter and velocity amplitude $Re = U_{max} D/v = 13\,325$. Turbulence is modelled by the SST eddy-viscosity two-equation model.

DOI: 10.1002/fld

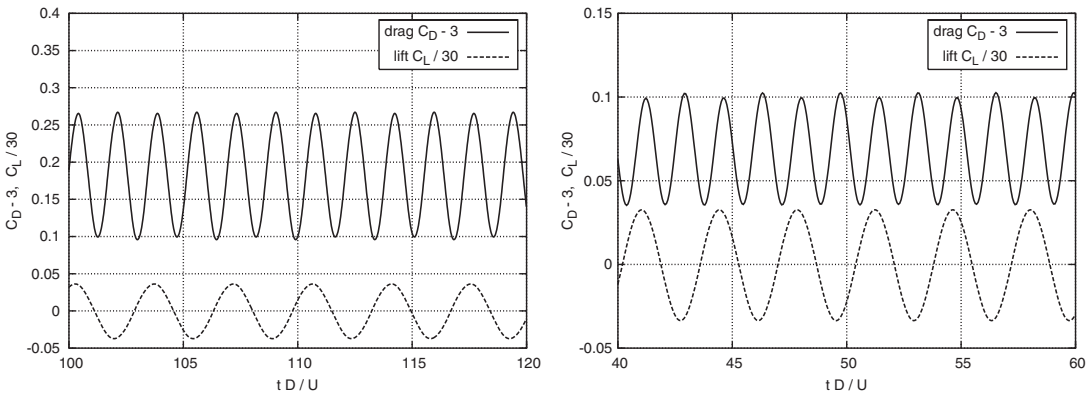

Figure 4. Laminar flow around cylinder, left: single time method with $\beta = 10U$ and right: dual time method.

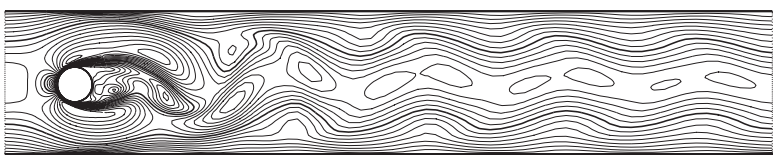

Figure 5. Instantaneous laminar flow around cylinder, dual time stepping. Isolines of velocity.

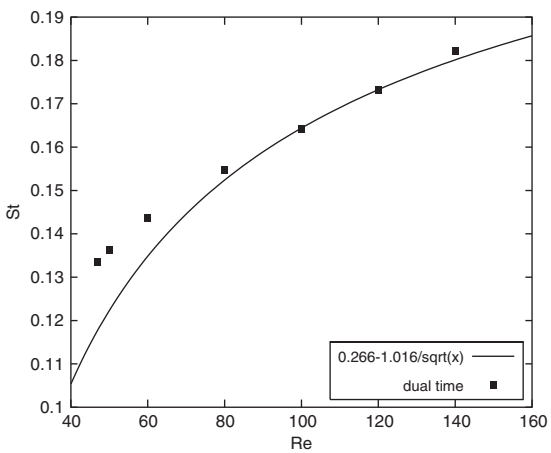

Figure 6. Reynolds number dependence of Strouhal number.

We used dual time stepping method with $\beta = U_{\max}$ and $\Delta t = \frac{1}{72}$ of forcing period $1/(75\,\text{Hz})$. The computed instantaneous velocity on jet axis is compared with measured [10] phase-averaged velocity in Figure 8. For larger x/D, the flowfield corresponds to steady free jet. Next, Figure 9

DOI: 10.1002/fld

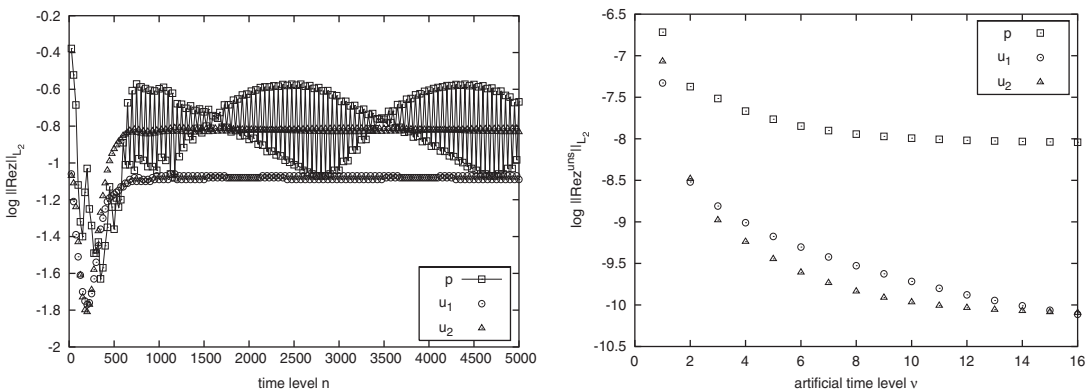

Figure 7. Convergence history for dual time method.

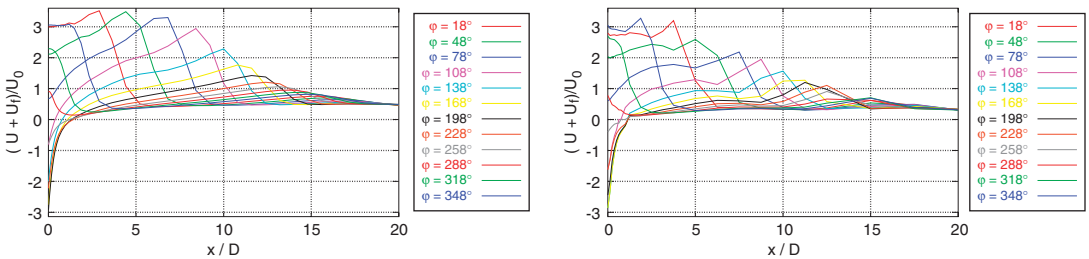

Figure 8. Phase-averaged velocity on jet axis, left: computation and right: measurement.

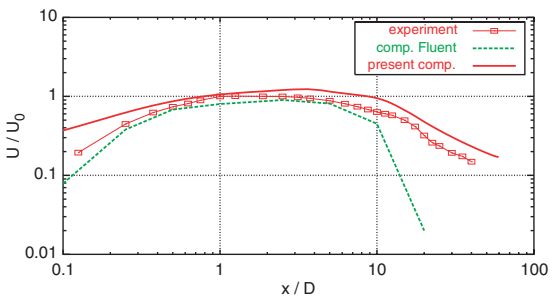

Figure 9. Time-averaged velocity on the jet axis.

shows time-averaged velocity on jet axis. The computational results achieved using Fluent code with axisymmetrical formulation in [10] are also shown. The velocity on the axis in Fluent decreases too fast, which suggests higher spreading rate than in the experiment. The time-averaged velocity profiles exhibit self-similarity already in the unsteady region. The computational results, Figure 10, have this feature except for small distance to the nozzle, where an approximate boundary condition

DOI: 10.1002/fld

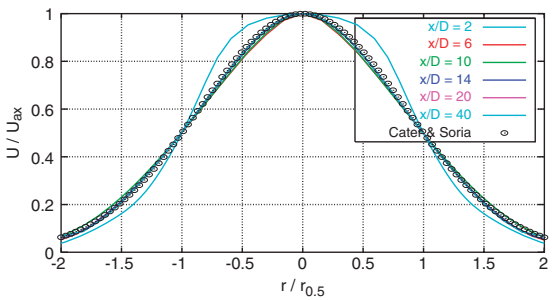

Figure 10. Time-averaged velocity profiles.

again plays a role. In this figure, the $r_{0.5}$ denotes the radial distance from jet axis, where the velocity reaches half of the axial velocity. Velocity profiles moreover agree well with empirical correlation $U/U_{\mathrm{ax}} = \exp[-\ln(2)(r/r_{0.5})^2]$ according to [11].

5. CONCLUSIONS

In this work, an artificial compressibility implicit upwind finite-volume method has been applied to steady and unsteady flows of incompressible Newtonian fluid. The unsteady cases included self-induced and forced unsteadiness. The steady simulation of 2D and 3D turbulent flows over confined backward-facing step shows that unlike eddy viscosity, the 3D EARSM model gives acceptable results due to ability to capture secondary flows. In the single time method, the magnitude of artificial compressibility parameter is limited from above from computational reasons and does not allow a reliable prediction of unsteady flow. The extension with dual time, on the other hand, works well for both laminar test cases as well as for simulation of turbulent free synthetic jet.

ACKNOWLEDGEMENTS

The work was partially supported by Grant No. 205/05/0005 of GA CR and Research plan MSM 6840770010.

REFERENCES

1. Kozel K, Louda P, Sváček P. Numerical solution of flow in backward facing step. In *Numerical Mathematics and Advanced Application*, Feistauer M, Dolejší V, Najzar K (eds). Springer: Heidelberg, 2004; 596–604.
2. Chorin AJ. A numerical method for solving incompressible viscous flow problems. *Journal of Computational Physics* 1967; **2**(1):12–26.
3. Menter FR. Two-equation eddy-viscosity turbulence models for engineering applications. *AIAA Journal* 1994; **32**(8):1598–1605.
4. Wallin S. Engineering turbulence modeling for CFD with a focus on explicit algebraic Reynolds stress models. *Ph.D. Thesis*, Royal Institute of Technology, Stockholm, 2000.
5. Hellsten A. New advanced k–ω turbulence model for high-lift aerodynamics. *AIAA Journal* 2005; **43**:1857–1869.
6. Turkel E. Algorithms for the Euler and Navier–Stokes equations for supercomputers. *Technical Report ICASE Report No. 85-11*, NASA, 1985.
7. Armaly BF, Durst F, Pereira JCF, Schönung B. Experimental and theoretical investigation of backward-facing step flow. *Journal of Fluid Mechanics* 1983; **127**:473–496.

DOI: 10.1002/fld

8. Schäfer M, Turek S. Benchmark computations of laminar flow around a cylinder. *NNFM 52 'Flow Simulation on High Performance Computers II'*. Vieweg: Braunschweig, 1996; 547–566.
9. Wang A-B, Trávníček Z, Chia K-C. On the relationship of effective Reynolds number and Strouhal number for the laminar vortex shedding of a heated circular cylinder. *Physics of Fluids* 2000; **12**(6):1401–1410.
10. Trávníček Z, Vogel J, Vít T, Maršík F. Flow field and mass transfer experimental and numerical studies of a synthetic impinging jet. *HEFAT2005*, *4th International Conference on Heat Transfer*, *Fluid Mechanics*, *and Thermodynamics*, Cairo, Egypt, 2005.
11. Cater JE, Soria J. The evolution of round zero-net-mass-flux jets. *Journal of Fluid Mechanics* 2002; **472**:167–200.

DOI: 10.1002/fld